Journal of Power Sources 182 (2008) 124–132

Contents lists available at ScienceDirect

Journal of Power Sources

journal homepage: www.elsevier.com/locate/jpowsour

Review

Recent advances in direct formic acid fuel cells (DFAFC)

Xingwen Yu, Peter G. Pickup*

Department of Chemistry, Memorial University of Newfoundland, St. John's, Newfoundland, Canada A1B 3X7

ARTICLE INFO

Article history:
Received 28 February 2008
Received in revised form 26 March 2008
Accepted 27 March 2008
Available online 3 April 2008

Keywords:
Direct formic acid fuel cell (DFAFC)
Formic acid oxidation
Catalyst
Crossover
Cell configuration

ABSTRACT

Polymer electrolyte membrane-based direct formic acid fuel cells (DFAFC) have been investigated for about a decade, and are now becoming an important area of portable power system research. DFAFCs have the advantages of high electromotive force (theoretical open circuit potential 1.48 V), limited fuel crossover, and reasonable power densities at low temperatures. This paper provides a review of recent advances in DFAFCs, mainly focussing on the anodic catalysts for the electro-oxidation of formic acid. The fundamental DFAFC chemistry, formic acid crossover through Nafion® membranes, and DFAFC configuration development are also presented.

Contents

1. Introduction

Polymer electrolyte membrane (PEM)-based fuel cells are generally considered as viable candidates to replace batteries in portable power devices. Traditionally, H_2-fed PEMFCs and direct methanol fuel cells (DMFCs) are the dominant choices [1–9]. However, despite many years of intensive research into these technologies, inherent limitations still remain.

The H_2-PEMFC is limited by the high cost of miniaturized hydrogen containers, the potential dangers in the transport and use of hydrogen, and its low gas-phase energy density. For DMFCs, liquid methanol has an impressive energy density (approximately 4900 Wh L^{-1}), but its electrocatalytic oxidation rate is very low relative to that of H_2. The limited compatibility of methanol with Nafion® membranes allows only low concentrations (generally 1–2 M) to be fed to a DMFC [3,10,11]. Exceeding this limit leads to a high rate of fuel crossover, which simultaneously reduces fuel utilization and decreases cell performance. In addition, the inherent toxicity of methanol, particularly in the vapor phase, remains an issue for commercialization of DMFC technology [9]. It is these limitations of hydrogen and methanol that have in recent years increased interest in direct formic acid fuel cells (DFAFCs) [12–38].

Formic acid is a liquid at room temperature and dilute formic acid is on the US Food and Drug Administration list of food additives that are generally recognized as safe [20]. Formic acid exhibits a smaller crossover flux through Nafion® than methanol [16,19], allowing the use of highly concentrated fuel solutions and thinner membranes in DFAFCs. DFAFCs also have a higher electromotive

* Corresponding author. Tel.: +1 709 737 8657.
E-mail address: ppickup@mun.ca (P.G. Pickup).

0378-7753/$ – see front matter © 2008 Elsevier B.V. All rights reserved.
doi:10.1016/j.jpowsour.2008.03.075

force (EMF), as calculated from the Gibbs free energy, than either hydrogen or direct methanol fuel cells [9].

In only a few years of research, DFAFC technology has shown electrocatalytic oxidation activity far superior to DMFCs and in some cases performances approaching those of H_2-PEM fuel cells [22]. The major disadvantage of formic acid as a fuel is that its volumetric energy density is only 2104 Wh L^{-1}, considerably lower than that of neat methanol. However, this disadvantage can be compensated for by using a high concentration of formic acid. Thus, for many systems, especially smaller power systems, the advantages of DFAFC can outweigh those of its primary direct-liquid fuel cell contender, the DMFC.

In this review, recent advances in DFAFC research are reviewed, with a focus on progresses that has been made on catalysts for formic acid electro-oxidation. The fundamental DFAFC chemistry, formic acid crossover through Nafion® membranes, and DFAFC configuration development are also discussed.

2. Fundamentals of DFAFC chemistry and the mechanism of electro-oxidation of formic acid

As with all polymer electrolyte membrane-based fuel cells, the direct formic acid fuel cell also uses an air cathode. Oxygen reduction, through a 4-electron reaction at the cathode, is usually facilitated by a platinum based catalyst. At the anode, direct oxidation of formic acid releases two electrons per molecule. The cathode, anode and overall reactions of a direct formic acid fuel cell are described as:

$$\text{Anode}: \quad HCOOH \rightarrow CO_2 + 2H^+ + 2e^-, \quad E^0 \sim -0.25\,\text{V(vs.SHE)} \tag{1}$$

$$\text{Cathode}: \quad 1/2O_2 + 2H^+ + 2e^- \rightarrow H_2O, \quad E^0 = 1.23\,\text{V(vs.SHE)} \tag{2}$$

$$\text{Overall}: \quad HCOOH + 1/2O_2 \rightarrow CO_2 + H_2O, \quad OCV \sim 1.48\,\text{V} \tag{3}$$

The direct formic acid fuel cell has a higher electromotive force (EMF) (open circuit voltage (OCV) ~ 1.48 V; values varies slightly depending on the source [e.g. 9,13,39]) than either hydrogen or direct methanol fuel cells. The theoretical energy density of formic acid is determined as: $2F \times OCV \times (MW)^{-1}$. From the molecular weight MW (kg mol^{-1}), open circuit potential OCV (V) and the Faraday constant (F = 96,485 C mol^{-1}), formic acid has the intrinsic energy density of 1725 Wh kg^{-1}. Considering the density of this liquid (1.22 kg L^{-1}), the theoretical energy density of formic acid can also be expressed as 2104 Wh L^{-1}.

Whereas the direct formic acid fuel cell has been investigated for only about 12 years (use of formic acid as the fuel for a PEM fuel cell was first reported in 1996 in Ref. [12]), the investigation of the mechanism of formic acid oxidation has a much longer history [40–48]. The most commonly accepted mechanism is the so-called 'parallel or dual pathway mechanism' [47]. Direct oxidation (pathway 1) occurs via a dehydrogenation reaction, without forming CO as a reaction intermediate:

$$\text{Pathway1}: \quad HCOOH \rightarrow CO_2 + 2H^+ + 2e^- \tag{4}$$

The second reaction pathway (pathway 2) forms adsorbed carbon monoxide (CO) as a reaction intermediate by dehydration:

$$\text{Pathway 2}: \quad HCOOH \rightarrow -CO_{ads} + H_2O \rightarrow CO_2 + 2H^+ + 2e^- \tag{5}$$

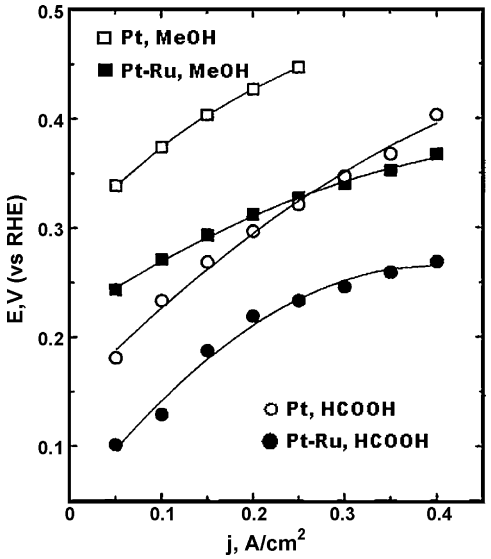

Fig. 1. Polarization curves for methanol and formic acid oxidation at Pt-black and Pt/Ru anodes. Cell operating conditions were: anode catalyst loading: 4 mg cm^{-2}, water/fuel mole ratio: 2, feed rate: 0.26 ml min^{-1}; cathode: Pt-black, 4 mg cm^{-2}, air feed rate: 10 ml min^{-1}; electrolyte: PBI membrane doped with H_3PO_4; temperature: 170 °C [12]. Reproduced by permission of The Electrochemical Society.

In reaction pathway 2, formic acid first adsorbs onto the catalyst surface forming an intermediate adsorbed CO species, which is then oxidized to the gaseous CO_2 end product. For direct formic acid fuel cells, dehydrogenation is the desired reaction pathway, to enhance overall cell efficiency and avoid poisoning of the catalyst. Anode catalyst selection is pivotal in directing formic acid oxidation to proceed via reaction pathway 1.

3. Anode catalysts for electro-oxidation of formic acid

3.1. Unsupported Pt-based catalysts

In the early stages of DFAFC development, Pt-based catalysts were employed in the anode layer. In the first report of a DFAFC [12], Weber et al. found that formic acid was electrochemically more active than methanol on both Pt-black and Pt/Ru catalysts. In addition, the Pt/Ru catalyst was more active than Pt-black for formic acid oxidation. The results are summarized in Fig. 1 [12]. Despite the significance of these results, there were surprisingly no further reports on DFAFCs until 2002, although interest in the fundamentals of formic acid electro-oxidation continued [47,48].

In 2002, a group of researchers at the University of Illinois again reported that formic acid is an excellent fuel for a fuel cell, and that formic acid fuel cells were attractive alternatives for small portable applications [13]. They used a proprietary Pt-based catalyst named as 'UIUC-B' in the anode layer to enhance the electro-oxidation of formic acid [13,14]. Currents up to 134 mA cm^{-2} and power outputs up to 48.8 mW cm^{-2} were obtained with their first DFAFC demonstration [13].

Following their successful implementation in the first DFAFC systems, Pt-based catalysts have been widely studied, and continue to be an important aspect of DFAFC anode catalyst research. Pt–M (M = a second metal other than platinum) bimetallic catalysts have been increasingly developed for DFAFCs [15,29,35,36,49]. Addition of a second metal not only reduces the use of platinum, but can also enhance the activity of the catalysts for the oxidation of formic acid. Pt/Ru, Pt/Pd, Pt/Au and Pt/Pb have recently been probed as the anode catalysts in DFAFCs, and the effects of Ru, Pd, Au, Pb on the catalytic activities have accordingly been examined. Waszczuk et

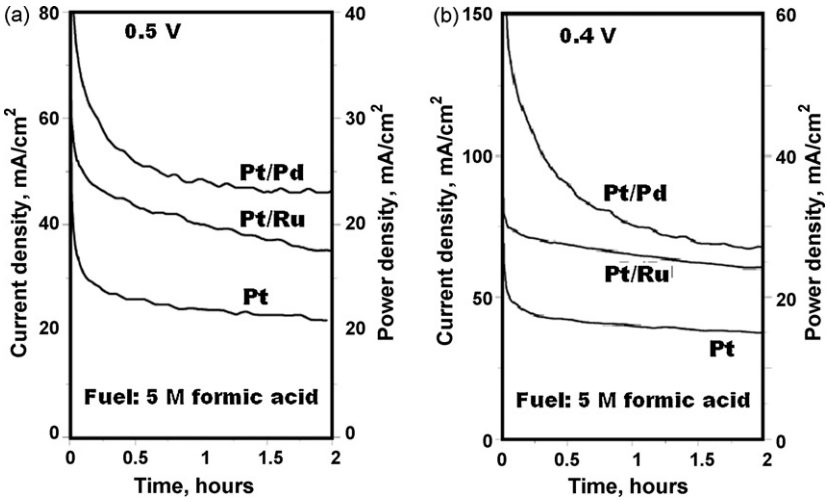

Fig. 2. Constant voltage tests on a DFAFC at cell potentials of (a) 0.5 V and (b) 0.4 V. Catalysts: platinum black, Pt/Ru, and Pt/Pd; fuel: 5 M formic acid at 0.2 ml min^{-1}; cell temperature: 30 °C. Reprinted from [15] with permission from Elsevier.

al. [49] synthesized a series of Pt-based catalysts by spontaneous deposition of Pd and/or Ru to decorate platinum nanoparticles. Decoration of the Pt surface with Pd provided the greatest increase in activity. Rice et al. [15] investigated these Ru and Pd decorated Pt catalysts in more detail, and a representative comparison of the DFAFC performances of the Pt-black, Pt/Ru and Pt/Pd catalysts is illustrated in Fig. 2 and in Table 1. Both Ru and Pd were found to significantly enhance the catalytic activity, with Pt/Pd providing the best performance at high cell potentials. Pt/Ru provided the best maximum power density of 70 mW cm^{-2}, but this was at a very low cell potential of 0.26 V. The rate of current decay also varied between catalysts, with Pt/Ru showing the fastest decay while the current at Pt/Pd became quite stable after an initial rapid decay. From a fundamental point of view, Rice et al. [15] proposed that addition of palladium to platinum enhanced the electro-oxidation rate of formic acid via a direct reaction mechanism (dehydrogenation pathway). This was studied further by Thomas and Masel [50], who showed that the energy barrier for decomposition of formic acid to CO_2 decreases with increasing palladium coverage. In contrast, addition of ruthenium appears to suppress the direct pathway and enhance the electro-oxidation of formic acid via a reactive CO intermediate (dehydration pathway) [15]. Thomas and Masel [50] found that there were no synergistic effects between platinum and palladium in a bimetallic Pt/Pd catalyst with respect to formic acid oxidation activity, and suggested that the improved activity was due to resistance to poisoning.

Choi et al. [29] studied an unsupported Pt–Au alloy prepared by borohydride reduction as an anode catalyst for formic acid oxidation in a DFAFC. From their study, compared with Pt–Ru, the Pt–Au catalyst showed a higher catalytic activity, as illustrated in Fig. 3. Moreover, the improved cell performance with the Pt–Au catalyst was also maintain during long-term operation of the cell. These authors proposed that the oxidation of formic acid on a Pt–Au catalyst occurs mainly through the direct dehydrogenation pathway, without significant formation of adsorbed CO [29].

A variety of intermetallic phases of Pt with Bi, Pb, In, Sn, Mn and Sb have been evaluated for formic acid oxidation, with PtBi, $PtBi_2$, PtPb, and PtIn being identified as the most promising candidates [51]. Surface treatment methods to improve the activities of PtBi and PtPb have been investigated [52], and methods for the synthesis of PtPb nanoparticles have been developed and compared [53,54]. A study of a Pt–Bi alloy produced by induction melting [55] revealed the importance of dissolution and underpotential deposition (upd) of Bi atoms at the surface, as well as the formation of Bi oxides. Surface modification of PtRu with irreversibly adsorbed Bi atoms increases its activity for formic acid oxidation, apparently by hindering CO adsorption on Pt sites [56].

Bimetallic PtPb prepared by arc-melting has been shown to provide much higher and more stable (over 1000 s) formic acid oxidation activity than Pt [57]. PtPb nanoparticle catalysts also show high activity for formic acid oxidation and more stable performance (over 9 h) than Pt, PtRu, and Pd [58].

The enhancement of formic acid oxidation by Bi (and As) has been attributed to the so-called 'third-body effect' in which the addition of a second element (third-body) to Pt reduces the number of adsorption sites for CO due to geometrical hindrance and their surface is poisoned by the adsorbed CO to a lesser extent than a pure Pt surface [59]. In contrast, the activity enhancement of Pt–Pb for formic acid oxidation has been attributed to an electronic interaction between Pb and Pt [60]. The high catalytic activity for a Bi

Table 1
Current density and power density comparison for DFAFCs with Pt, Pt–Ru and Pt–Pd anode catalysts running at voltages of 0.4 and 0.5 V [15]

	Current density (mA cm^{-2})		Power density (mW cm^{-2})	
	0.4 V	0.5 V	0.4 V	0.5 V
Pt	37.44	22.02	15.69	10.30
Pt–Ru	60.61	35.14	25.40	16.44
Pt–Pd	67.32	46.39	28.24	21.71

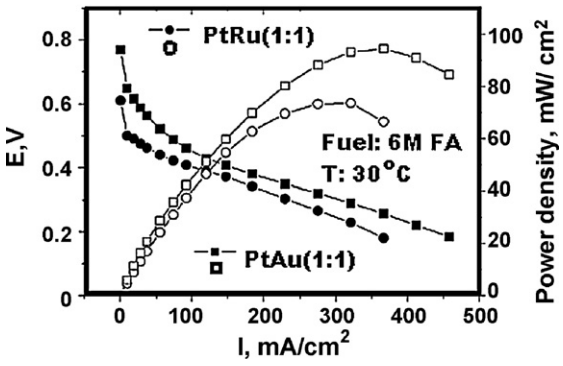

Fig. 3. Single cell performances of PtAu-based and PtRu-based MEAs with 6 M formic acid and oxygen at 30 °C. Reprinted from [29] with permission from Elsevier.

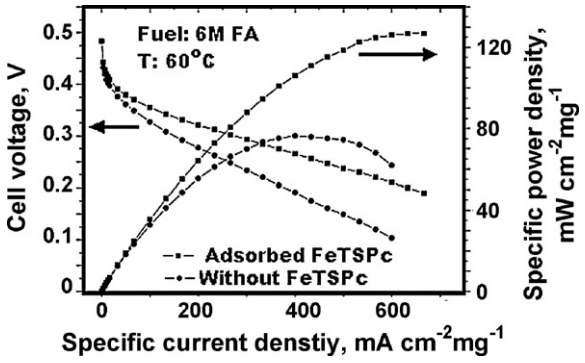

Fig. 4. Polarization curves for a DFAFC before and after adsorption of FeTSPc on the anode. Specific current density is 'current density/Pt loading'. The cell was operated at 60 °C and atmospheric pressure with 6 M formic acid. Anode: Pt loading 0.5 mg cm^{-2}, fuel flow rate 1.0 ml min^{-1}; cathode: Pt loading 1.5 mg cm^{-2}, 100 sccm of dry oxygen. Reprinted from [35] with permission from Elsevier.

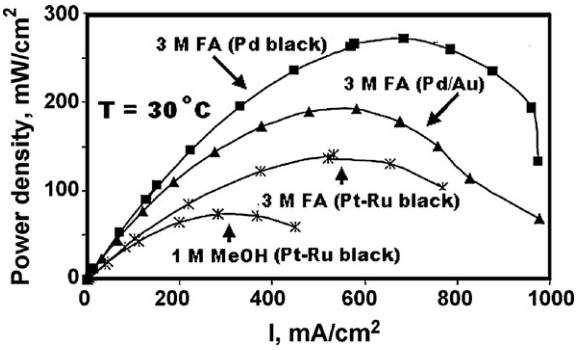

Fig. 5. Power density curves for fuel cells fed with 1 M methanol, 3 M formic acid and hydrogen gas. Flow rates of methanol, formic acid and hydrogen were 1 ml min^{-1}, 3.5 ml min^{-1} and 200 sccm, respectively. Dry air was supplied to the cathode at a flow rate of 390 sccm. The cell operation temperature was 30 °C. Anodic catalysts used in the cell are indicated, while a Pt-black catalyst was used for cathode [20]. Copyright Wiley-VCH Verlag GmbH & Co. KGaA. Reproduced with permission.

modified Pt catalyst has also been explained by electronic effects working in addition to a 'third-body effect' [61].

The fundamental mechanism of formic acid oxidation remains an important and challenging topic, and has been intensively studied by employing Pt single crystals modified with up to a monolayer of a second metal. Arenz et al. [62,63] have investigated the Pt(1 1 1)–Pd system in detail as well as Pt–Pd alloy single crystals. Pd atoms at the surface were found to be 3–5 times more active than Pt atoms at 0.4 V. FTIR revealed that CO adsorbed on the Pt sites, but not the Pd sites. Macia et al. [61] have studied the effects of Bi adlayers on formic acid oxidation at stationary and rotating Pt(1 1 1) electrodes. Activity increased with increasing Bi coverage up to 0.1–0.25 of a monolayer, depending on the formic acid concentration. Current–time transients indicated that no poisoning occurred for the modified electrodes. It was proposed that the reaction proceeds through adsorbed formate as an intermediate without significant accumulation of adsorbed CO.

A Pt_4Mo alloy has also been shown to possess high activity for formic acid oxidation [64]. The formation of a hydrous Mo oxide on the surface was found to decrease poisoning by absorbed CO, and may also increase the rate of the direct pathway for formic acid oxidation.

From a theoretical point of view, Demirci [65] has predicted that the Pt–Ag bimetallic system might be a promising catalyst for DFAFCs, but there have not yet been any experimental studies to investigate this hypothesis.

Recently, an interesting Pt–FeTSPc (tetrasulfophthalocyanine) co-catalyst for the electro-oxidation of formic acid was developed [35]. The enhancement of cell performance by using the FeTSPc modified Pt catalyst is shown in Fig. 4. The authors proposed that the enhanced activity with the FeTSPc was due to a combination steric hindrance inhibiting the formation of adsorbed CO, and an intrinsic kinetic enhancement due to electron donation by the FeTSPc [35].

3.2. Unsupported Pd-based catalysts

Electro-oxidation of formic acid on Pd catalysts has been extensively studied [41,66–69]. Use of pure Pd as the anode catalyst in DFAFCs was first reported by Ha et al. [20]. Compared with Pt-based catalysts, the Pd-black generated unusually high power densities at ambient (22 °C) and higher (30–50 °C) temperatures. A representative comparison between Pd black, Pd–Au, and Pt–Ru is shown in Fig. 5. Ha et al. [20] found that the activity of the Pd black catalyst decreased with the cell operation time, with a consequent loss of DFAFC performance. However, the lost activity could largely be recovered by applying a high anodic potential. The same group also studied the effects of operating temperature and formic acid concentration on the performances of a DFAFC with a Pd anode, a DFAFC with a Pt–Ru anode, a DMFC (direct methanol fuel cell) with a Pt–Ru anode and a H_2/air fuel cell [22]. The results are summarized in Table 2. The DFAFC with the Pd anode catalyst not only generated much higher power density than either the DFAFC or DMFC using the Pt–Ru catalyst, but also approached the performance of the hydrogen-PEM fuel cell. Deactivation of the Pd catalyst was a problem for the DFAFCs, particularly when operated with high formic acid concentrations, but again it was found that the initial cell performance could be recovered by applying a potential of 1.2 V to the anode for a few seconds [22].

The deactivation of Pd black during formic acid oxidation in a DFAFC has recently been investigated by impedance spectroscopy [70]. The anode Nyquist plots consisted of irregular arcs indicating that several processes contributed to the impedance. The width of the arcs increased during deactivation and this was attributed to an

Table 2
Comparison of power densities for different types of fuel cell, and power densities of DFAFCs under different operating conditions [22]

Fuel cell	Anode catalyst	Temperature (°C)	Fuel concentration (M)	Peak power density (mW cm^{-2})
H_2-air	Pd	20	–	320
MeOH-air	Pt–Ru	20	1.0	50
FA-air	Pt–Ru	20	3.0	84
FA-air	Pd	20	3.0	253
FA-air	Pd	30	3.0	300
FA-air	Pd	40	3.0	350
FA-air	Pd	50	3.0	375
FA-air	Pd	20	10.0	255
FA-air	Pd	20	15.0	230
FA-air	Pd	20	20.0	103

Table 3
Recent syntheses of Pd/C and Pd–M/C catalysts with impregnation methodologies

Catalyst	Precursor	Reducing agent	Additive	Reference
Pd/C	$PdCl_2$	$NaBH_4$	–	[21,73]
Pd/C	$PdCl_2$	Ethylene glycol	–	[26]
Pd/C	$PdCl_2$	$NaBH_4$	H_3BO_3, NH_4F	[27]
Pd–Pt/C	H_2PtCl_6, $(NH_4)_2PdCl_6$	Methanol	SB12*	[74]
Pd–P/C	$PdCl_2$, NaH_2PO_2	$NaBH_4$	H_3BO_3, NH_4F	[28]

SB12*: 3-(*N*,*N*-dimethyldodecylammonio)propanesulfonate.

increasing charge transfer resistance. The charge transfer resistance also increased with increasing concentration of formic acid. It was speculated that poisoning of the anode with an unknown, non-CO, organic species occurred during deactivation.

The poisoning of DFAFC catalyst by impurities in the fuel has been documented in a recent UK patent and US patent application [71]. Methyl formate and acetic acid where shown to produce significantly enhanced degradation rates at concentrations above 10 and 1000 ppm, respectively. A method based on freezing the best commercial formic acid is described for producing a "preferred fuel".

3.3. Carbon-supported Pt-based and Pd-based catalysts

The attractive features of high electrical conductivity, chemical stability and low cost have led to the extensive application of high surface-area carbon materials as supports for precious metal fuel cell catalysts, in order to reduce the noble metal loading and reduce the system cost [72]. Lovic et al. [39] demonstrated that the kinetics of formic acid oxidation on Pt/C catalysts were consistent with those on pure platinum, with the reaction occurring via the dual pathway mechanism comprising direct dehydrogenation of HCOOH as the main reaction and formation of poisoning species as a parallel reaction.

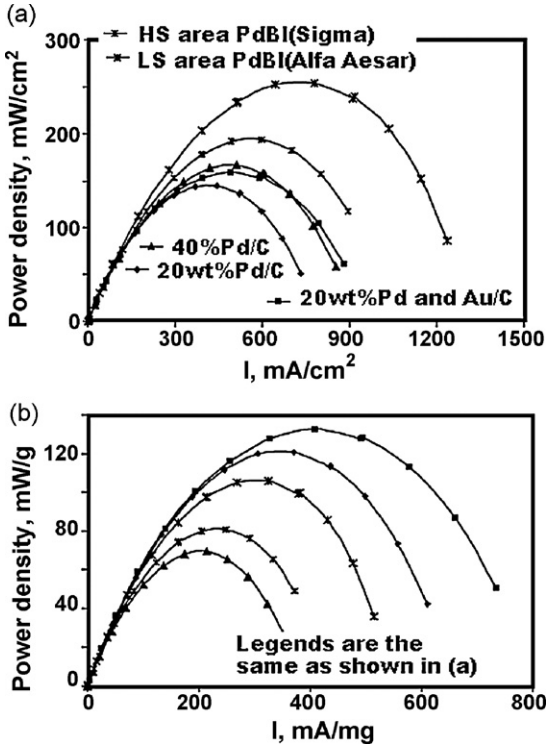

Fig. 6. Power density plots (a) per membrane surface area and (b) per total catalyst mass, for a direct formic acid fuel cell with various Pd anode catalysts operating with dry air at 30 °C with 5 M formic acid. Reprinted from [73] with permission from Elsevier.

Carbon supported palladium catalysts have become a very important area in DFAFC catalyst research in recent years [21,26–28,73,74], demonstrating good activity along with the potential for more efficient palladium metal utilization and lower metal loadings. Pd/C or Pd–M/C (M = a second metal other than Pd) catalysts are generally obtained through chemical solution phase impregnation syntheses. Recent advances in Pd/C and Pd–M/C catalyst syntheses are summarized in Table 3.

Ha et al. [21] successfully synthesized finely dispersed Pd particles on a Vulcan XC-72® carbon support, with palladium loadings of 20 and 40 wt%. Using these two Pd/C catalysts, DFAFCs generated a maximum power density of 145 mW cm^{-2} (with 20% Pd/C) and 172 mW cm^{-2} (with 40% Pd/C), as summarized in Fig. 6a [73]. Results for the carbon-supported catalysts were compared with those for pure palladium in a DFAFC. Although the total power density generated by the 20% Pd/C catalyst was lower, the power density per unit mass of noble metal was much higher than for the Pd black catalyst, as summarized in Fig. 6b. In addition to the benefits of higher palladium utilization efficiency, it was also found that the Pd/C catalysts showed less deactivation than for pure palladium during operation of the cell, especially for high concentrations of formic acid [21]. Larsen et al. [73] reported that the addition of gold to Pd/C can further improve the activity of the catalyst, and these results are also summarized in Fig. 6.

Liu et al. [26] synthesized a Pd/C catalyst by a microwave-assisted polyol process, and this was reported to yield a high power density in a DFAFC. Fig. 7 shows a representative performance comparison between single DFAFC cells prepared with the Pt/C

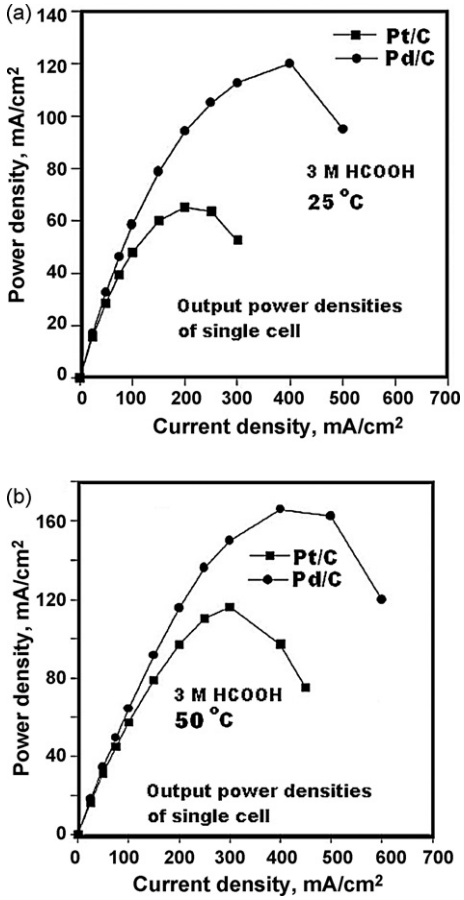

Fig. 7. Output power densities for a single cell operating at (a) 25 °C and (b) 50 °C. Anode: Pt/C or Pd/C (8 mg cm^{-2}), 3 M HCOOH, 2 ml min^{-1}. Cathode: Pt/C (E-TEK) (4 mg cm^{-2}), O_2 500 cm^3 min^{-1}. Reprinted from [26] with permission from Elsevier.

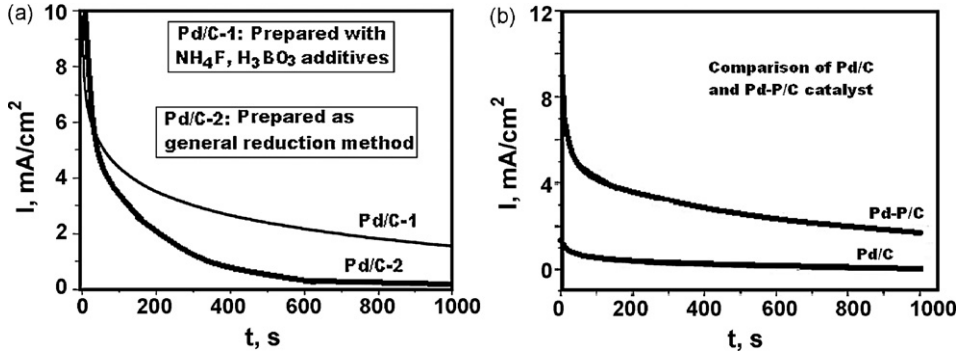

Fig. 8. Chronoamperometric curves for oxidation of 0.5 M HCOOH in 0.5 M H_2SO_4 solution on various Pd/C catalyst electrodes. (a) Comparison of Pd/C catalysts prepared with or without NH_4F, H_3BO_3 additives. Fixed potential: 0.10 V [27]; (b) comparison of Pd/C and Pd–P/C catalyst electrodes. Fixed potential: 0.3 V [28]. Reprinted from [27,28] with permission from Elsevier.

and Pd/C catalysts synthesized by this microwave-assisted process [26].

Zhang et al. [27] reported an aqueous solution phase synthesis of a Pd/C catalyst with NH_4F and H_3BO_3 as additives. NH_4F forms a complex with $PdCl_2$ and this promotes the formation of finely dispersed Pd particles with smaller average sizes (3.2 nm) and relatively less crystallinity. Consequently, the catalytic activity and stability of the Pd/C catalyst synthesized in the presence of NH_4F were enhanced. A representative result is shown in Fig. 8a. Zhang et al. [28] also reported a Pd–P/C catalyst prepared via a solution phase synthesis with NaH_2PO_2 as a co-precursor. Combining palladium with the non-metal element phosphorus improved both the activity and stability of the catalyst as illustrated in Fig. 8b.

Li and Hsing [74] developed a novel synthesis method for a carbon supported Pd–Pt catalyst using the surfactant 3-(*N*,*N*-dimethyldodecylammonio)propanesulfonate (SB12) as the stabilizer. Compared with a commercial (E-TEK) $Pt_{0.5}Pd_{0.5}$/C catalyst, the SB12 stabilized Pt–Pd/C catalysts have the advantages of better Pt–Pd dispersion and higher catalytic performance [74].

Uhm et al. [36] studied Pt–Pb catalysts obtained by modifying supported platinum electrodes with upd lead. The Pt–Pb_{upd} catalysts showed higher electrocatalytic activities than pure platinum or Pt–Ru catalysts. Furthermore, a Pt/Pb_{upd}/Pt multi-layer anode structure was shown to provide an enhanced cell performance that was stable over a 5 h period of evaluation [36]. Pt modified Au nanoparticles supported on carbon have also been found to be effective for formic acid oxidation [75].

3.4. Other supporting tactics for Pt-based and Pd-based catalysts

In addition to carbon, preparation of platinum or palladium based catalysts on other supporting substrates has also been recently reported. Yi et al. [76] developed a novel titanium-supported nanoporous bimetallic Pt–Ir/Ti catalyst by a hydrothermal process, and with H_2PtCl_6 and $IrCl_3$ as the precursors, and formaldehyde as the reduction agent. Compared to pure platinum, the titanium-supported Pt–Ir catalysts have a significantly higher catalytic activity for formic acid oxidation. The authors proposed that electro-oxidation of formic acid on Pt–Ir catalysts followed the dehydration pathway via a 'CO' intermediate.

Highly active palladium based catalysts tend to be passivated under DFAFC conditions, which leads to a decay of the DFAFC performance with the cell operation time. In order to obtain highly stable palladium catalysts, Larsen et al. [77] studied the stability of palladium deposited as a sub-monolayer on various metal foil supports such as V, Mo, W, and Au. Among the metal foil supported catalysts, Pd–V has the best stability, as summarized in Fig. 9. In the

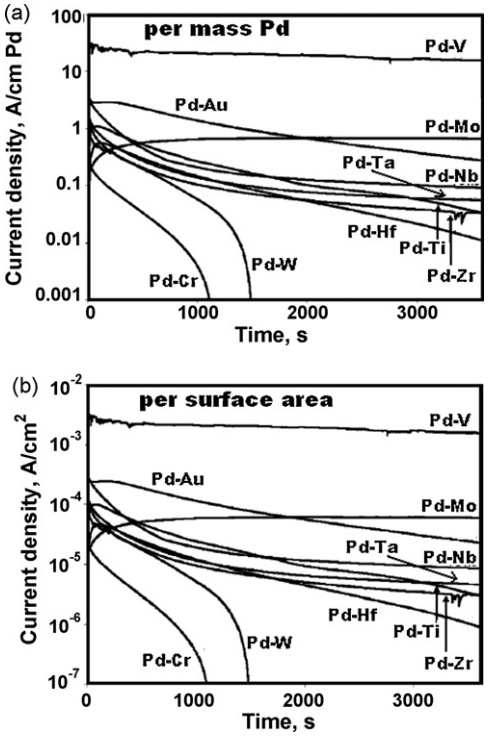

Fig. 9. Chronoamperometric activity of Pd–M catalysts at 0.3 V vs. RHE, (a) per mass of Pd; (b) per surface area with θ_{Pd} = 0.6 (M = Ti, Zr, Hf, V, Nb, Ta, Cr, Mo, W, Au). The *I*–*t* curves were measured in a solution containing 5 M HCOOH and 0.1 M H_2SO_4 [77]. Reproduced by permission of The Electrochemical Society.

authors' opinion, the results obtained for these Pd/metal foil catalysts provide important information for the development of highly stable palladium based catalysts by alloying a second metal phase, such as vanadium.

4. Crossover of formic acid through Nafion® membranes

For any type of PEM-based fuel cell, the fuel fed to the negative electrode (anode) can permeate the membrane to the positive electrode (cathode). This phenomenon reduces fuel utilization, results in a detrimental mixed potential, competes for and potentially poisons the cathode catalyst and thereby decreases the efficiency of the oxygen reduction reaction [78,79]. For liquid fuels it can also cause flooding of the cathode catalyst layer [79].

One of the claimed advantages of formic acid for use in PEM fuel cells is low crossover through Nafion® membranes. However,

Table 4
Fluxes (10^{-8} mol cm^{-2} s) of formic acid through Nafion® membranes [16]

	Formic acid concentration (M)			
	1	5	10	20
Nafion® 117	2.03 ± 0.07	12.3 ± 0.3	18.6 ± 1.1	17.0 ± 1.2
Nafion® 112	5.49 ± 9.37	40.6 ± 4.0	45.7 ± 3.9	34.7 ± 2.6

this does not mean that the crossover of formic acid is negligible, and crossover is still a significant issue limiting the performance of DFAFCs.

Recently, a number of studies have been performed to examine and quantify the crossover behavior of formic acid in DFAFCs [16,19,33,80]. Rhee et al. [16] studied the permeation of formic acid through Nafion® 112 and Nafion 117 membranes at room temperature, their results are as summarized in Table 4. Wang et al. [19] studied formic acid crossover through a Nafion® 115 membrane at different temperatures and formic acid concentrations. Generally, the flux of formic acid through a Nafion membrane increases with increasing formic acid concentration and temperature [16,19]. Rhee et al. [16] demonstrated that the permeation of formic acid is higher through Nafion® 112 (50 μm) than through the thicker 180 μm Nafion® 117.

Jeong et al. [33] studied the crossover of formic acid in a real DFAFC operating environment under various operating conditions. The crossover behavior of formic acid was similar to that under the non-fuel cell conditions used by Rhee et al. [16] and Wang et al. [19]. As summarized in Fig. 10, crossover of formic acid increases with increasing formic acid concentration, but decreases with increasing current density as more formic acid is consumed at the anode. Methanol crossover was found to be ca. 6 times greater than that of formic acid under the same cell operating conditions, when expressed in terms of the crossover current (i.e. the current required to oxidize the fuel reaching the cathode) [33]. When fluxes (mol cm^{-2} s^{-1}) are compared, the difference is only a factor of two [19,33] or less [80], because oxidation of formic acid to CO_2 requires only two electrons while oxidation of methanol requires six electrons. This is contrary to Rhee et al.'s [16] original report of a two order of magnitude difference because they used an inaccurate crossover value for methanol in their comparison.

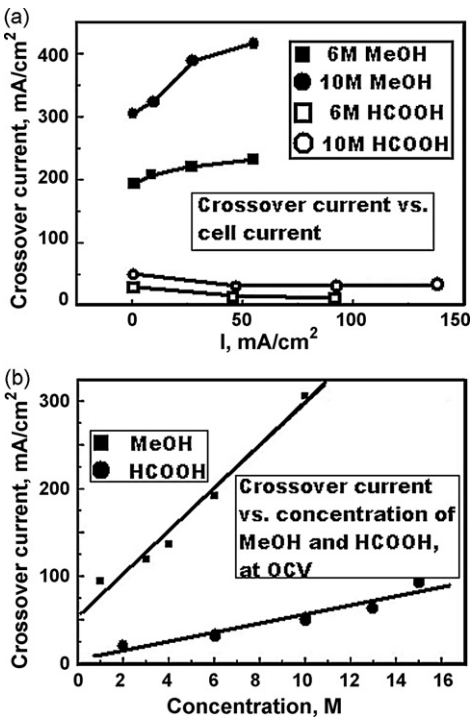

Fig. 10. Comparison of crossover fluxes for methanol and formic acid. (a) Crossover current under load vs. cell current for different concentration of MeOH and HCOOH; (b) crossover current vs. concentration of MeOH and HCOOH, at OCV. Reprinted from [33] with permission from Elsevier.

5. DFAFCs designs

Direct formic acid fuel cells are generally considered as attractive alternatives to replace batteries in portable power devices. For this purpose, most DFAFCs are designed as small portable fuel cells. In 2004, Ha et al. [17] successfully demonstrated a 2 cm × 2.4 cm × 1.4 cm passive miniature air breathing DFAFC. This cell operated very well with a wide range of formic acid concentrations and generated a current density of up to 250 mA cm^{-2} and a maximum power density of 33 mW cm^{-2}. After this first successful invention, this group also illustrated three different types of DFAFCs: (1) an active DFAFC, (2) an active air breathing DFAFC, and (3) a passive air breathing DFAFC [30]. In the active DFAFC, the formic acid was supplied to the anode by a liquid pump, and the air was supplied to the cathode by using a compressed gas cylinder. For the air breathing DFAFC, the cathode was exposed to ambient air instead of using a cathode flow field. For the passive DFAFC, the cathode was the same as in the air breathing cell, and the anode flow field was replaced by a fuel reservoir. In this passive DFAFC, formic acid was delivered from the fuel reservoir to the anode catalyst layer simply by diffusion and capillary action [30].

Yeom et al. [24,31] developed a microscale silicon-based direct formic acid fuel cell by using an integrated microscale membrane electrode assembly. In this cell design, the Nafion membrane was bonded between two silicon mesh electrodes which served as the catalyst support, current collector, and structural elements. With this cell, they demonstrated two types of DFAFCs with different air (or oxygen) delivery modes. In a forced oxygen flow mode, the cell generated a maximum power density of ca. 30 mW cm^{-2} at room temperature; a value thought to be limited by mass transfer to the anode. In a air-passive mode with quiescent air at the cathode, the cell generated a maximum power density of 12.3 mW cm^{-2}, now thought to be limited by oxygen transport to the anode [31].

As traditional low temperature fuel cells, DFAFC were originally designed by using Nafion membranes as the electrolyte. In 2006, Chu et al. [25] reported that a nanoporous silicon could also be used as the proton conducting membrane material for membrane electrode assemblies in microscale silicon fuel cells, and successfully demonstrated a silicon membrane based DFAFC. However, in this cell, addition of a small amount of sulfuric acid (0.5 M in this demonstration) to the formic acid fuel was necessary to increase proton conductivity.

Chen et al. [34] reported a novel design for a membraneless micro-DFAFC by employing a planar microchannel. This theoretical design is based on the fundamentals of hydrokinetics and hydrodynamics of flowing liquids: that the two liquid streams can be separated by the nature of laminar flow within the microchannel under small Reynolds number. The air (or oxygen) at the cathode would need to be dissolved in an aqueous solution (sulfuric acid suggested in Chen's design) to flow as a liquid stream. They propose that the fuel (formic acid) and air (or oxygen) liquid streams flowing in parallel through the planar microchannel can be kept separate without the need of a membrane by controlling the flow rate of the liquid streams, and the shape and length of the microchannel [34].

6. Conclusions

This paper reviews recent advances in direct formic acid fuel cells, including the fundamental DFAFC chemistry, anodic catalysts for formic acid oxidation, formic acid crossover through Nafion® membranes, and DFAFC configuration development.

The DFAFC has a high theoretical open circuit voltage (OCV = 1.48 V) due to the low standard potential of formic acid. Formic acid oxidation generally follows the so-called 'dual pathway' mechanism involving both a dehydrogenation process leading to direct formation of CO_2 and a dehydration process forming a 'CO' intermediate which is further oxidized to the gaseous CO_2 end product.

Platinum-based and palladium-based catalysts are commonly used in DFAFC development, with use of Pd becoming more prevalent. A series of Pt-based bimetallic systems including Pt–Ru, PtBi, PtPd, PtAu, PtPb, PtIr have been reported as effective catalysts for DFAFCs. Pd-based catalysts generally have higher activity for formic acid oxidation, but tend to become less active with cell operation time. Applying a high potential to the anode can overcome this drawback by regenerating most of the catalyst's original activity. Carbon supported palladium-based catalysts have become an important topic of research in recent years. A variety of syntheses routes for Pd/C (or Pd–M/C) catalysts have been reported, and the synthesized catalysts show high palladium utilization efficiency and high catalytic activity for DFAFC operation.

Formic acid has good compatibility with Nafion membranes. Crossover behavior and the recent quantification studies of formic acid fluxes through Nafion membranes are summarized. These results show that the formic acid crossover flux is only about a factor of two smaller than for methanol. However, the smaller number of electrons involved in formic acid oxidation (2 vs. 6) cause the effect of formic acid crossover on the performance of the cathode to be much smaller than for methanol.

DFAFCs are generally considered as attractive portable power devices, and are designed as small portable fuel cells. Varieties of both passive and active miniature DFAFCs have been demonstrated and run successfully with a wide range of formic acid concentrations. Other DFAFC designs summarized in this paper include a silicon-based Nafion® membrane miniature DFAFC, silicon membrane miniature DFAFC, and a theoretical membraneless DFAFC design.

The demand for power sources with superior performance has increased as a result of the rapid growth of the portable electronics market. There is great potential for micro-fuel cells to deliver more energy per volume and weight than conventional batteries. DFAFCs appear to be attractive candidates for meeting increasing power density demands. With the advantages of high electromotive force, limited fuel crossover, and high practical power densities at low temperature, DFAFC are a very promising power source for the near future.

References

[1] W. Vielstich, H.A. Gasteiger, A. Lamm (Eds.), Handbook of Fuel Cells, Wiley, New York, 2003.
[2] L. Carrette, K.A. Friedrich, U. Stimming, Chemphyschem. 1 (2000) 162.
[3] A.S. Arico, S. Srinivasan, V. Antonucci, Fuel Cells 1 (2001) 133.
[4] G.J.K. Acres, J. Power Sources 100 (2001) 60.
[5] C. Stone, A.E. Morrison, Solid State Ionics 151 (2003) 1.
[6] M. Winter, R.J. Brodd, Chem. Rev. 104 (2004) 4245.
[7] C.C. Chan, Proc. IEEE 95 (2007) 704.
[8] R. von Helmolt, U. Eberle, J. Power Sources 165 (2007) 833.
[9] U.B. Demirci, J. Power Sources 169 (2007) 239.
[10] S.Q. Song, V. Maragou, P. Tsiakaras, J. Fuel Cell Sci. Technol. 4 (2007) 203.
[11] V. Neburchilov, J. Martin, H.J. Wang, J.J. Zhang, J. Power Sources 169 (2007) 221.
[12] M. Weber, J.T. Wang, S. Wasmus, R.F. Savinell, J. Electrochem. Soc. 143 (1996) L158.
[13] C. Rice, R.I. Ha, R.I. Masel, P. Waszczuk, A. Wieckowski, T. Barnard, J. Power Sources 111 (2002) 83.
[14] S. Ha, C.A. Rice, R.I. Masel, A. Wieckowski, J. Power Sources 112 (2002) 655.
[15] C. Rice, S. Ha, R.I. Masel, A. Wieckowski, J. Power Sources 115 (2003) 229.
[16] Y.W. Rhee, S.Y. Ha, R.I. Masel, J. Power Sources 117 (2003) 35.
[17] S. Ha, B. Adams, R.I. Masel, J. Power Sources 128 (2004) 119.
[18] Y.M. Zhu, S.Y. Ha, R.I. Masel, J. Power Sources 130 (2004) 8.
[19] X. Wang, J.M. Hu, I.M. Hsing, J. Electroanal. Chem. 562 (2004) 73.
[20] S. Ha, R. Larsen, Y. Zhu, R.I. Masel, Fuel Cells 4 (2004) 337.
[21] S. Ha, R. Larsen, R.I. Masel, J. Power Sources 144 (2005) 28.
[22] Y.M. Zhu, Z. Khan, R.I. Masel, J. Power Sources 139 (2005) 15.
[23] R.S. Jayashree, J.S. Spendelow, J. Yeom, C. Rastogi, M.A. Shannon, P.J.A. Kenis, Electrochim. Acta 50 (2005) 4674.
[24] J. Yeom, G.Z. Mozsgai, B.R. Flachsbart, E.R. Choban, A. Asthana, M.A. Shannon, R. Kenis, Sens. Actuators B: Chem. 107 (2005) 882.
[25] K.L. Chu, S. Gold, V. Subramanian, C. Lu, M.A. Shannon, R.I. Masel, J. Microelectromech. Syst. 15 (2006) 671.
[26] Z.L. Liu, L. Hong, M.P. Tham, T.H. Lim, H.X. Jiang, J. Power Sources 161 (2006) 831.
[27] L.L. Zhang, T.H. Lu, J.C. Bao, Y.W. Tang, C. Li, Electrochem. Commun. 8 (2006) 1625.
[28] L.L. Zhang, Y.W. Tang, J.C. Bao, T.H. Lu, C. Li, J. Power Sources 162 (2006) 177.
[29] J.H. Choi, K.J. Jeong, Y. Dong, J. Han, T.H. Lim, J.S. Lee, Y.E. Sung, J. Power Sources 163 (2006) 71.
[30] S. Ha, Z. Dunbar, R.I. Masel, J. Power Sources 158 (2006) 129.
[31] J. Yeom, R.S. Jayashree, C. Rastogi, M.A. Shannon, P.J.A. Kenis, J. Power Sources 160 (2006) 1058.
[32] C.M. Miesse, W.S. Jung, K.J. Jeong, J.K. Lee, J. Lee, J. Han, S.P. Yoon, S.W. Nam, T.H. Lim, S.A. Hong, J. Power Sources 162 (2006) 532.
[33] K.J. Jeong, C.A. Miesse, J.H. Choi, J. Lee, J. Han, S.P. Yoon, S.W. Nam, T.H. Lim, T.G. Lee, J. Power Sources 168 (2007) 119.
[34] F.L. Chen, M.H. Chang, M.K. Lin, Electrochim. Acta 52 (2007) 2506.
[35] X.C. Zhou, W. Xing, C.P. Liu, T.H. Lu, Electrochem. Commun. 9 (2007) 1469.
[36] S.Y. Uhm, S.T. Chung, J.Y. Lee, Electrochem. Commun. 9 (2007) 2027.
[37] A. Kundu, J.H. Jang, J.H. Gil, C.R. Jung, H.R. Lee, S.H. Kim, B. Ku, Y.S. Oh, J. Power Sources 170 (2007) 67.
[38] W. Chen, Y.W. Tang, J.C. Bao, Y. Gao, C.P. Liu, W. Xing, T.H. Lu, J. Power Sources 167 (2007) 315.
[39] J.D. Lovic, A.V. Tripkovic, S.L.J. Gojkovic, K.D. Popovic, D.V. Tripkovic, P. Olszewski, A. Kowal, J. Electroanal. Chem. 581 (2005) 294.
[40] A. Capon, R. Parsons, J. Electroanal. Chem. 44 (1973) 1.
[41] A. Capon, R. Parsons, J. Electroanal. Chem. 44 (1973) 239.
[42] A. Capon, R. Parsons, J. Electroanal. Chem. 45 (1973) 205.
[43] R. Parsons, T.J. VanderNoot, J. Electroanal. Chem. 257 (1988) 9.
[44] N.M. Markovic, H.A. Gasteiger, P.N. Ross Jr., X.D. Jiang, I. Villegas, M.J. Weaver, Electrochim. Acta 40 (1995) 91.
[45] P.N. Ross, in: J. Lipkowski, P.N. Ross (Eds.), Electrocatalysis, Wiley-VCH, New York, 1998, pp. 43–74.
[46] T.D. Javi, E.M. Stuve, in: J. Lipkowski, P.N. Ross (Eds.), Electrocatalysis, Wiley-VCH, New York, 1998, pp. 75–154.
[47] J.M. Feliu, E. Herrero, in: W. Vielstich, H.A. Gasteiger, A. Lamm (Eds.), Handbook of Fuel Cells, vol. 2, Wiley, New York, 2003, p. 679.
[48] P. Waszczuk, A. Crown, S. Mitrovski, A. Wieckowski, in: W. Vielstich, H.A. Gasteiger, A. Lamm (Eds.), Handbook of Fuel Cells—Fundamentals, Technology and Applications, vol. 2, Wiley, New York, 2003, p. 635.
[49] P. Waszczuk, T.M. Barnard, C. Rice, R.I. Masel, A. Wieckowski, Electrochem. Commun. 4 (2002) 599.
[50] F.S. Thomas, R.I. Masel, Surf. Sci. 573 (2004) 169.
[51] E. Casado-Rivera, D.J. Volpe, L. Alden, C. Lind, C. Downie, T. Vazquez-Alvarez, A.C.D. Angelo, F.J. DiSalvo, H.D. Abruna, J. Am. Chem. Soc. 126 (2004) 4043.
[52] D. Volpe, E. Casado-Rivera, L. Alden, C. Lind, K. Hagerdon, C. Downie, C. Korzeniewski, F.J. DiSalvo, H.D. Abruna, J. Electrochem. Soc. 151 (2004) A971.
[53] L.R. Alden, D.K. Han, F. Matsumoto, H.D. Abruna, F.J. DiSalvo, Chem. Mater. 18 (2006) 5591.
[54] L.R. Alden, C. Roychowdhury, F. Matsumoto, D.K. Han, V.B. Zeldovich, H.D. Abruna, F.J. DiSalvo, Langmuir 22 (2006) 10465.
[55] A.V. Tripkovic, K.D. Popovic, R.M. Stevanovic, R. Socha, A. Kowal, Electrochem. Commun. 8 (2006) 1492.
[56] A.V. Tripkovic, S.L. Gojkovic, K.D. Popovic, J.D. Lovic, A. Kowal, Electrochim. Acta 53 (2007) 887.
[57] L.J. Zhang, Z.Y. Wang, D.G. Xia, J. Alloys Compd. 426 (2006) 268.
[58] F. Matsumoto, C. Roychowdhury, F.J. DiSalvo, H.D. Abruna, J. Electrochem. Soc. 155 (2008) B148.
[59] E. Herrero, A. Fernandez-Vega, J.M. Feliu, A. Aldez, J. Electroanal. Chem. 350 (1993) 73.
[60] X. Xia, T. Iwasita, J. Electrochem. Soc. 140 (1993) 2559.
[61] M.D. Macia, E. Herrero, J.M. Feliu, J. Electroanal. Chem. 554 (2003) 25.
[62] M. Arenz, V. Stamenkovic, T.J. Schmidt, K. Wandelt, P.N. Ross, N.M. Markovic, Phys. Chem. Chem. Phys. 5 (2003) 4242.
[63] M. Arenz, V. Stamenkovic, P.N. Ross, N.M. Markovic, Surf. Sci. 573 (2004) 57.
[64] S.L. Gojkovic, A.V. Tripkovic, R.M. Stevanovic, N.V. Krstajic, Langmuir 23 (2007) 12760.
[65] U.B. Demirci, J. Power Sources 173 (2007) 11.
[66] M. Baldauf, D.M. Kolb, J. Phys. Chem. 100 (1996) 11375.
[67] M. Tian, B.E. Conway, J. Electroanal. Chem. 581 (2005) 176.

[68] N. Hoshi, K. Kida, M. Nakamura, M. Nakada, K. Osada, J. Phys. Chem. B 110 (2006) 12480.
[69] W.P. Zhou, A. Lewera, R. Larsen, R.I. Masel, P.S. Bagus, A. Wieckowski, J. Phys. Chem. B 110 (2006) 13393.
[70] W.S. Jung, J.H. Han, S. Ha, J. Power Sources 173 (2007) 53.
[71] R.I. Masel, Y. Zhu, Z. Khan, M. Man, UK Patent GB2424650B (2007) and US Patent Application 20,060,059,769 (2006).
[72] H.S. Liu, C.J. Song, L. Zhang, J.J. Zhang, H.J. Wang, D.P. Wilkinson, J. Power Sources 155 (2006) 95.
[73] R. Larsen, S. Ha, J. Zakzeski, R.I. Masel, J. Power Sources 157 (2006) 78.
[74] X.G. Li, I.M. Hsing, Electrochim. Acta 51 (2006) 3477.
[75] I.S. Park, K.S. Lee, J.H. Choi, H.Y. Park, Y.E. Sung, J. Phys. Chem. C 111 (2007) 19126.
[76] Q.F. Yi, A.C. Chen, W. Huang, J.J. Zhang, X.P. Liu, G.R. Xu, Z.H. Zhou, Electrochem. Commun. 9 (2007) 1513.
[77] R. Larsen, J. Zakzeski, R.I. Masel, Electrochem. Solid State Lett. 8 (2005) A291.
[78] A. Heinzel, V.M. Barragan, J. Power Sources 84 (1999) 70.
[79] K.M. McGrath, G.K.S. Prakash, G.A. Olah, J. Ind. Eng. Chem. 10 (2004) 1063.
[80] C. Song, M. Khanfar, P.G. Pickup, J. Appl. Electrochem. 36 (2006) 339.